Nanomaterial-Enabled Photovoltaic and Photovoltaic–Thermal Systems: Recent Advances, Critical Challenges, and Future Perspectives a Review

***Amenah Radhi Hamad, **Ali Al-Jubainawi**

*The General Directorate of Misan Education, Ministry of Education, Iraq

**Department of Mechanical Engineering, College of Engineering, University of Misan, Maysan, Iraq

[1]*Date of Receiving: 28 September 2026; Date of Acceptance: 31 October 2026; Date of Publication: 15 November 2026*

Abstract

In order to enhance the electrical and thermal performance of photovoltaic-thermal (PVT) collectors as well as photovoltaic (PV) power conversion, nanomaterial engineering offers complementary routes. Performance determined using identical control setups, consistent system boundaries, and long term validation is generally absent from the descriptions of improvements; instead, they are expressed in terms of specific optical, electrical, or heat transfer properties. Nanostructured silicon, passivating and carrier selective interfaces, quantum dots, anti-soiling coatings, single and hybrid nanofluids, nano-enhanced phase change materials, and perovskite tandem devices are all part of this critical narrative review. It also consolidates chosen modeling studies. Considering fluctuations in illuminated area, operational temperature, flow conditions, useful-heat supply, and auxiliary energy usage, interventions are specified in terms of their functional location and regulatory mechanism. Instead of evidence of improvement from specific nanoparticles, technological standards depend on independently verified solar-cell efficiency statistics. Studies on controlled PVT have shown configuration-dependent benefits from hybrid nanofluids and thermal storage, but negative exergy results and effective non-nano phase-change controls imply that thermal conductivity or aggregate first-law efficiency cannot prove system-level superiority on their own. Therefore, we offer an evidence-to-deployment methodology that is integrated and places an emphasis on matched controls, calibrated measurements, net electrical output, usable thermal energy, exergy, operational stability, manufacturability, and life-cycle implications. Additional research is required to address the following areas: scalable functional interfaces, anti-soiling solutions tailored to the local climate, stable coolants at low concentrations, and long-term field validation. Nanomaterials' potential practical applications, according to the review, must be demonstrated at the interfaces of relevant devices, collectors, and whole-life systems.

Keywords: *Nanomaterials; photovoltaic cells; photovoltaic–thermal collectors; hybrid nanofluids; interfacial passivation; phase-change materials*

Nomenclature and abbreviations

1. **Abbreviations**

Abbrev.	Definition	Abbrev.	Definition
AR	Antireflection	MWCNT	Multiwalled carbon nanotube
CNT	Carbon nanotube	NEPCM	Nano-enhanced phase-change material

[1] How to cite the article: Hamad A.R., Al-Jubainawi A.; (November 2026); Nanomaterial-Enabled Photovoltaic and Photovoltaic–Thermal Systems: Recent Advances, Critical Challenges, and Future Perspectives a Review; *International Journal of Universal Science and Engineering*; Vol 13, 147-169

Abbrev.	Definition	Abbrev.	Definition
DSC	Differential scanning calorimetry	PCM	Phase-change material
EQE	External quantum efficiency	PCE	Power conversion efficiency
FF	Fill factor	PDMS	Polydimethylsiloxane
GO	Graphene oxide	PV	Photovoltaic
IEC	International Electrotechnical Commission	PVT (PV/T)	Photovoltaic–thermal
ISOS	International Summit on Organic Photovoltaic Stability (test protocols)	rGO	Reduced graphene oxide
ITO	Indium tin oxide	TPV	Thermophotovoltaic (outside the scope of this review)
J–V	Current density–voltage characteristic	UPS	Ultraviolet photoelectron spectroscopy
LCOE	Levelized cost of electricity	UV	Ultraviolet
MPP	Maximum power point	XPS	X-ray photoelectron spectroscopy

2. Nomenclature (symbols and units)

Symbol	Definition	Unit
A	Illuminated cell area or collector reference area	m^2
c_p	Specific heat capacity of the working fluid	J kg^{-1} K^{-1}
FF	Fill factor	–
G	Incident solar irradiance	W m^{-2}
h	Specific enthalpy in the flow-exergy expression	J kg^{-1}
h_c	Convective heat-transfer coefficient	W m^{-2} K^{-1}
Jsc	Short-circuit current density	A m^{-2} or mA cm^{-2}
k	Thermal conductivity	W m^{-1} K^{-1}
$\dot{m}$	Coolant mass flow rate	kg s^{-1}
Paux	Auxiliary electrical power excluding pump power	W
Pmax	Maximum PV electrical power	W
Pnet	Net electrical power delivered by the system	W
PPV	Gross electrical power generated by the PV module	W
Ppump	Electrical power required by the coolant pump	W
$\dot{Q}u$	Rate of useful thermal energy delivery	W
s	Specific entropy in the flow-exergy expression	J kg^{-1} K^{-1}
T_0	Ambient reference (dead-state) temperature	K
Tin	Coolant inlet temperature	K
Tlm	Representative thermodynamic mean heat-delivery temperature	K
Tout	Coolant outlet temperature	K
Voc	Open-circuit voltage	V
$\dot{V}$	Volumetric flow rate	m^3 s^{-1}
Δp	Pressure drop across the coolant flow circuit	Pa
ΔT	Temperature difference	K or °C
ηe	PV electrical conversion efficiency	– or %
ηex	Exergy efficiency (boundary must be specified)	– or %
ηpump	Pump efficiency	–
ηth	PVT useful-thermal efficiency	– or %
ηtotal	First-law total PVT efficiency, ηe + ηth	– or %
μ	Dynamic viscosity of the coolant	Pa s
ρ	Coolant density	kg m^{-3}

1. Introduction

Photovoltaic (PV) technologies have evolved beyond incremental improvements in absorber materials toward increasingly precise control of optical, electronic, and interfacial losses. Progress is now evaluated not only through power-conversion efficiency (PCE), but also through operational stability, reproducibility, manufacturability, and

electricity generation under realistic environmental conditions. The independently verified Solar Cell Efficiency Tables (Version 68) reported efficiencies of 28.1% for a large-area crystalline-silicon research cell and 35.2% for a perovskite/silicon multijunction research cell [1]. These findings show where technology is going, yet neither of them can be explained by a single nanomaterial. Not to mention that commercial-module performance or annual energy yield are not directly equal to efficiencies certified for small-area laboratory devices under specified lighting and temperature circumstances. Hence, in order to conduct a thorough evaluation of nano-enabled PV technologies, it is necessary to take into account material-level attributes, verified device characteristics, and performance advantages at the system or module level.

There are a lot of interconnected limitations in solar energy conversion that can be circumvented with nanostructured materials. The optical path length, reflection, and scattering are all affected by the surface textures, dielectric structures, and selected metallic nanostructures within the absorber. A combination of carrier-selective contacts and ultrathin passivation layers can enable charge extraction while simultaneously inhibiting interfacial recombination. More options for adjusting spectrum absorption and energy-level alignment are made available by nanocrystalline absorbers and tailored heterointerfaces. When evaluating performance based on a single material quality, the trade-offs inherent in these systems are often not apparent. For instance, black-silicon texturing can significantly reduce front-surface reflection while simultaneously increasing the electrically active interfacial area; so, for optimal device performance, appropriate passivation is essential [2]. In a similar vein, passivating-contact systems must find a middle ground between inefficient majority-carrier transport and limited minority-carrier recombination [3]. Therefore, an increase in absorptance or carrier mobility does not necessarily lead to a proportional increase in stable PCE. Instead, interpretation needs a concurrent consideration of the short-circuit current density, open-circuit voltage, fill factor, spectrum response and device-to-device variability.

The physics of solar devices adds a different scale of thermal management assessment. In typical modules only a proportion of the incident solar radiation is converted to electricity. A large portion of the solar energy is converted to module heating or dispersed via other channels. The increased cell temperature might decrease the conversion efficiency and expedite some breakdown mechanisms especially when operating in hot climes. Photovoltaic–thermal (PVT or PV/T) collectors combine a PV laminate with a thermal recovery circuit to produce energy and possibly beneficial low or medium temperature heat. Other potential heat-transfer media, including dispersions of metal oxides, carbon-based nanomaterials, or numerous particle ingredients have been investigated. However, the increase in the effective thermal conductivity is not sufficient to achieve an improvement at the collector level. The performance of the net depends on viscosity, stability of dispersion, geometry of the channels, flow regime, pressure losses, electricity of the pumping and temperature at which useful heat is given. Energy and exergy analyses can consequently yield different interpretations: one PVT investigation identified nanofluid configurations associated with lower electrical exergy performance [4]. Furthermore, time-dependent changes in colloidal stability and fluid properties complicate extrapolation from freshly prepared laboratory suspensions to continuously circulating systems [5], a concern also discussed in reviews of nano-enhanced PVT cooling [6].

Phase-change materials (PCMs) provide a complementary strategy for passive or hybrid thermal regulation. Through latent-heat absorption during melting, a PCM can attenuate transient PV temperature peaks and postpone heat release until periods of reduced solar input. Nanoparticulate fillers, including boron nitride and carbon-based structures, may improve thermal transport within the storage medium; however, these improvements can coincide with reductions in latent-heat capacity per unit composite mass, particle segregation, or changes in behavior during repeated melting and solidification. Experimental studies of boron-nitride-enhanced PCM systems show that the filler loading, PCM composition and geometrical arrangement should be tuned simultaneously rather than selecting only to maximize the thermal conductivity [7]. Recent literature stresses the importance of the preparation processes, their complete characterization and linked thermophysical properties for the assessment of nano-enhanced PCMs for PV thermal control [8]. Critically, the incremental contribution of a nanoparticle additive can be isolated only when nano-PCM systems are compared to an untreated PV configuration and a PCM-only control of geometric equivalence.

The wide variety of possible nanomaterials further adds to the difficulty of drawing broad conclusions from published results. Many different types of nanostructures exist, each with its own unique optical response, chemical stability,

charge-transport characteristics, processing compatibility, environmental effect, and graphene derivatives, carbon nanotubes, plasmonic metals, quantum dots, two-dimensional semiconductors, and perovskites. Parasitic metal absorption or additional recombination routes can result from improper placement of plasmonic devices, which can enhance local electromagnetic fields or redirect incident radiation [9]. The device performance in perovskite structures may be more affected by meticulous interfacial engineering than by the nominal concentration of nanoparticles. Reduced interfacial defects and improved charge extraction have been associated with the formation of atomically coherent interlayers on SnO 2 electron-transport electrodes, for instance [10]. Thus, material identity is insufficient to rank performances. Any comparison should also take into account morphology, surface functionalization, layer position, thickness or concentration, device design, fabrication technique and the strength of the causa1 evidence supporting the observed improvement.

Although considerable gains have been made, the available evidence is still very varied and often poorly standardized to support sound engineering judgments. PV studies may report peak PCE, increased absorption, or short-duration stable operation. PVT studies often focus on temperature reduction, thermal efficiency, or combined energy efficiency. In certain studies, a nanofluid-cooled PVT collector is compared with an uncooled PV module, thereby confusing the general benefit of incorporating active cooling with the incremental effect of nanoparticle addition. Comparability of nominally comparable performance indicators is further compromised by differences in aperture area, irradiance, flow conditions, thermal boundary definitions and temperature of recovered heat. A defensible synthesis must, therefore, discriminate between independently certified cell records, laboratory device tests, outdoor collector experiments, thermophysical-property data, and numerical predictions. It must also distinguish between absolute efficiency, percentage point differences and relative percentage improvements. In the absence of such methodological discipline, perceived improvements may be due to inconsistent experimental bounds rather than true changes in material or system performance.

Thus, the key knowledge gap is not due to a lack of literature on nanostructured PV surfaces, nanofluid-based cooling, or nano-enhanced thermal storage individually. Rather, these research fields have seldom been integrated into an evidence framework that follows the nanoscale material mechanisms to practical electrical generation, useful thermal delivery, auxiliary-energy-adjusted output, heat quality, operational reliability, and life-cycle consequences. An improved optical response associated with a faster degradation cannot be seen as a clear improvement, as well as an increase of the convective heat transfer associated with disproportionate hydraulic losses. Neither can the certified efficiency of a tandem laboratory cell be confused with the annual yield of an integrated PVT system. Therefore, a cross-scale analytical approach is needed to determine which relationships are physically transferable from materials to devices and systems, and which findings are architecture-, comparator- and operating environment-specific.

This review addresses this gap with four objectives: (i) classification of nanomaterial strategies by their physical mechanism and location within PV and PVT architectures; (ii) critical evaluation of experimentally demonstrated optical, electrical, thermal, and exergy outcomes in light of appropriate non-nano or otherwise matched reference configurations; (iii) assessment of engineering limitations in terms of pumping demand, agglomeration, degradation, fabrication scalability, costs, and environmental impacts; and (iv) development of reporting priorities and research directions for improved reproducibility and technology translation. The paper first presents the review technique and evidence hierarchy, and then examines basic enhancement mechanisms and applications in established and new PV devices. The following sections explore PVT cooling, PCM integration, spectrum splitting, material characterisation, performance normalization, reliability and techno-economic evaluation. A consolidated research path is presented next. Solar PV and PVT systems are discussed. Thermophotovoltaic (TPV) converters, which produce energy from thermal radiation from a high-temperature source, are not included.

2. Review methodology and evidence assessment

The present study is a structured critical narrative-review, not a systematic review or meta-analytic design. The literature searches were focused and included primary experimental studies, representative numerical studies, seminal contributions, and selected benchmark or consensus papers available up to October 2026. Search concepts included photovoltaic conversion, photovoltaic-thermal collectors, nanostructures, nanoparticles, nanofluids, phase change materials, perovskites, interfacial passivation, nanocoatings, light control, exergy, hydraulic power, reliability and

techno-economic assessment. Articles maintained by publishers and DOI metadata were favored above secondary summaries, when available. Publications were considered relevant if they explicitly identified a material intervention, its claimed physical process, and at least one measurable performance or durability outcome. Studies with traditional water cooling or unmodified PCM were also retained if they represented necessary non-nano reference settings.

The search technique applied is given in enough detail to identify the main themes but an archived bibliographic export, a comprehensive deduplication record and a complete title/abstract screening log were not provided. Therefore, the present review does not report the total number of records found or excluded, nor does it present a PRISMA flow diagram, pooled effect estimate or meta-analytic measure of certainty. The evidence was grouped into independently validated device performance, controlled laboratory experimentation, outdoor experimentation, thermophysical-property characterization, numerical modeling, or review/consensus recommendations. Reported results were evaluated within their individual experimental contexts, expressly distinguishing between efficiency reported as a percentage, an absolute percentage-point difference, and a relative % change.

The evidentiary strength of each reported enhancement was assessed by four criteria: (i) the suitability of the reference configuration, including uncooled PV, water-cooled PVT, and non-nano PCM controls; (ii) the completeness of the description of the operating conditions including device area, irradiance, temperature, spectrum, and fluid flow; (iii) the availability of uncertainty estimates, repeated measurements, auxiliary-energy accounting, and stability observations; and (iv) the alignment between the scale of the evidence and the scale of the conclusion, from materials and cells to modules and deployed systems. This hierarchy avoids laboratory certification findings from being presented as annual module yields and short-duration tests being taken as proof of service lifespan. The comparative approach and design advice we offer are not novel experimental discoveries, but rather critical synthesis.

Selection was also guided by relevance to four complementary evidence domains: (a) nanoscale optical and electronic interfaces in PV devices; (b) experimental performance data of nano-enabled PVT collectors; (c) benchmarks for conventional and modified thermal storage; and (d) guidance on measurement, stability and durability. The parameters and test limits presented in the original research are retained in the evidence tables . Experimental observations are clearly separated from modeled outcomes . Record-setting PV efficiencies are considered as independently confirmed benchmarks for full device architectures, and not individual nanoparticle impacts. The source selection was purposeful rather than exhaustive and hence formal risk-of-bias scores, pooled effect estimates and claims of total literature coverage are not warranted.

3. Mechanisms and nanomaterial placement

3.1 Optical mechanisms

The absorption of incident radiation, which is dependent on the wavelength, and the spatial distribution of electromagnetic fields are modified by optical nanostructuring. For example, texturing of crystalline silicon alters interfacial reflection and angular scattering, yet the increase of surface area might lead to higher electronic losses. Metallic plasmonic structures may be used to increase near field intensity or to steer photons into an absorber. However, such advantages may be compensated by parasitic absorption and nonradiative quenching if the particle geometry or placement is not optimal [9]. Dielectric and photonic structures can offer alternate ways for light control with differing penalties for absorption, while anti-reflection and anti-soiling coatings can retain the optical flux incident on the active layer. Critically, a rise in absorptance, by itself, cannot establish an improvement in external quantum efficiency or electrical output, especially when carrier extraction is limiting.

3.2 Electronic mechanisms

You may tune the orientation of the energy band, decrease nonradiative recombination at crucial interfaces, and minimize the densities of electrically active defects by using nanoscale interlayers. Photoluminescence intensity and lifetime, quasi-Fermi-level splitting, transient photovoltage or photocurrent, impedance spectroscopy, calibrated current-voltage characteristics, external quantum efficiency, and large feature sizes alone should not be used to infer their function; complementary measurements are required. The purpose of passivating connections

in crystalline silicon is to suppress minority carriers while collecting majority carriers efficiently [3]. Perovskite devices also rely on spatially homogenous surfaces and chemically selective defect passivation [10,11,12,13]. If the interlayer creates a transport barrier that is too thick or misaligned, the reduction in surface recombination could be nullified by insufficient charge extraction.

3.3 Thermal mechanisms

The thermal power recovered for liquid cooled PVT systems depends on the coolant mass flow rate, specific heat capacity and temperature rise across the collector. The presence of suspended nanoparticles can change the effective conductivity, viscosity, heat capacity, and, for optically active fluids, the absorption characteristics. These features do not directly lead to an increase in the efficiency of the collector, which also depends on the geometry of the heat exchanger, the convective regime, the operating temperature, the heat transfer area and the pumping demand. Conductive fillers or networks can expedite the charging and discharging of nano-enhanced PCMs, however they may decrease the amount of latent-heat-storing material, increase segregation or change the supercooling behavior . Spectral-selective PVT setups exhibit another trade-off – a nanofluid or filter can be used to intercept specified wavelengths upstream of the PV device, but the filtering must be matched to the absorber bandgap and thermal-service needs to minimize needless photocurrent losses [14].

3.4 Material-placement taxonomy

A useful taxonomy for nanomaterials should specify both the chemistry and the location of the function: (A) front-glass or anti-soiling coatings; (B) absorber textures and active layers; (C) electron- or hole-selective interfaces; (D) back contacts and encapsulation; (E) rear thermal-contact layers or exchanger surfaces; (F) circulating nanofluids; (G) nano-enhanced thermal-storage composites; and (H) spectral-splitting fluids or optical elements. These same ingredients can be used for very different jobs in these places. For example, TiO2 nanostructures provide high-area electron-transport frameworks for dye-sensitized cells, but TiO2 particles dispersed in PVT coolants mainly influence thermophysical behavior and fluid stability, rather than photovoltaic charge generation [4,15]. Fig. 1. Summary of the main functional sites of nanomaterial interventions. Fig. 2. Representative photovoltaic and photovoltaic–thermal systems.

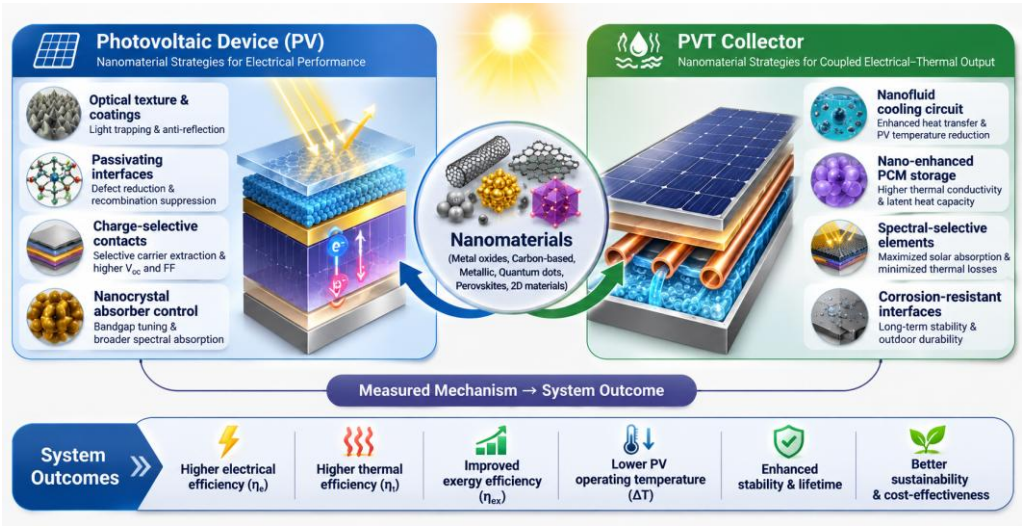


Fig. 1. Functional locations of nanomaterial interventions within PV devices and PVT collectors. Original conceptual synthesis; arrows indicate proposed functional relationships rather than experimentally measured causal effects.

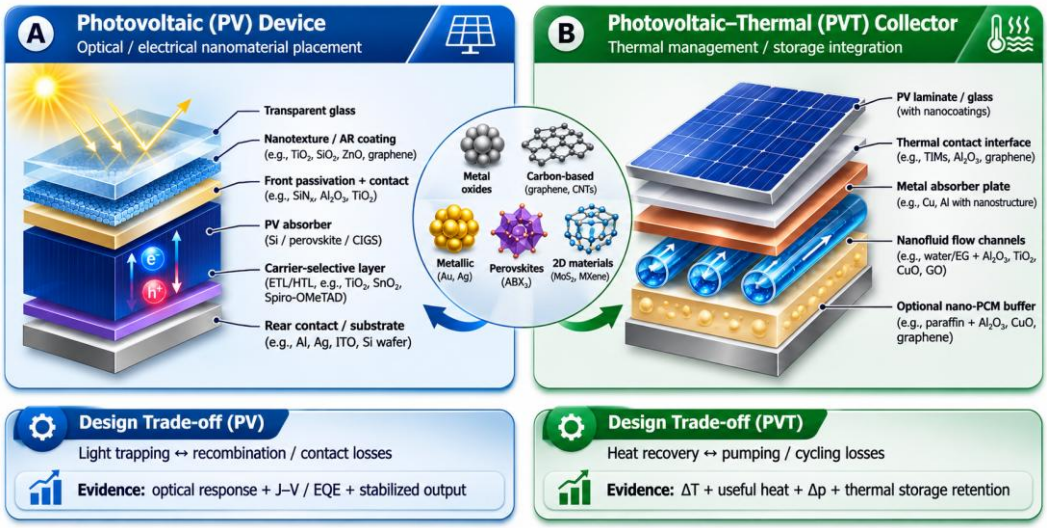


Fig. 2. Schematic cross-sections indicating the location of nanoscale functions in PV and PVT architectures (not to scale). Absorber layers, carrier-selective interfaces, and front coatings serve PV functions, whereas rear thermal interfaces, nanofluid passages, and optional nano-enhanced PCM components contribute to PVT heat recovery. The illustrated components are not intended to represent one simultaneously realized device.

Fig. 2 illustrates why the functional position of a nanomaterial is integral to performance attribution. Surface texturing and interfacial passivation should be evaluated using optical and electrical diagnostics, whereas colloidal additives and nano-enhanced storage composites require thermal, hydraulic, cycling, and durability measurements. The depicted cross-sections are conceptual architectures and should not be interpreted as experimentally realized layer stacks.

4. Nanomaterials in silicon and emerging PV technologies

4.1 Crystalline silicon

The black-silicon structures demonstrate the trade-offs inherent in nanoscale surface engineering. Savin et al. addressed the recombination linked to the expanded textured surface and achieved 22.1% efficiency in an interdigitated-back-contact black-silicon device [2]. This result is an interesting historical demonstration, not the contemporary silicon efficiency limit. More contemporary architectures are more and more based on improved electrical contacts and surface passivation: for instance, a hybrid-back-contact silicon device in 2025 obtained a PCE of 27.81% and a fill factor of 87.55% by combining passivation and laser processed tunneling contacts [16]. Taken together, these results suggest that the minimization of optical reflection is as critical as the suppression of contact-related carrier losses in advanced crystalline-silicon photovoltaics.

4.2 Metal-oxide electron-selective interfaces

SnO2 and TiO2 should be considered on the basis of their real interfacial roles and not only as light-harvesting additions. These oxides are mostly used as electron-transport layers or interface modifiers for various perovskite devices. The atomically coherent interlayers reported by Min et al. on SnO2 electrodes highlight the critical role of interfacial order and defect management [10]. Relevant material attributes are energy-level alignment, trap density, carrier selectivity, chemical compatibility and processing temperature. ZnO can give good electron-transport properties, however interactions with certain perovskite compositions can affect interfacial stability, therefore claims of universal performance cannot be justified. In dye-sensitized solar cells, nanoporous TiO 2 is a high-area scaffold for dye adsorption and electron transport, and visible-light absorption is mostly the role of the sensitizing dye [15].

4.3 Perovskite/silicon and all-perovskite tandems

Liu et al. reported a stabilized independently validated efficiency of 33.89% for a perovskite/silicon tandem with bilayer interfacial passivation [11]. Most recently, flexible perovskite/silicon tandems have reached a certified efficiency of 33.6% and have shown a reported 91% retention of the initial efficiency after 5,000 bending cycles and a T80 of more than 2,000 h under the stipulated test conditions [12]. These results are evidence of a major step forward in device design and targeted stability testing, although mechanical cycling and controlled illumination in the lab are

not themselves sufficient to demonstrate multi-decade outdoor module performance. Research on tandem stability has also included all-inorganic perovskite structures and dipolar interface-passivation techniques [17,18].

4.4 Process scale and compositional control

A 2026 study of blade coating of ambient-air perovskite cells showed certified efficiencies of 26.5% for single-junction cells, 23.2% for modules, and 33.0% for perovskite/silicon tandems, indicating the importance of functional polymer interfaces for scalable processing [13]. Two-dimensional perovskite interlayers and chemical methods to inhibit oxidation in ambient manufacturing are complementary concepts [19,20]. Collectively, these results demonstrate that relevance for manufacturing requires not only good small-area PCE but also retention of performance during area scaling, film deposition, encapsulation, and continuous operation.

4.5 Carbon electrodes and 2D materials

Graphene, reduced graphene oxide, carbon nanotubes and MXene family compounds are often called electrically useful additives. However, their applicability for a specific device depends on significant changes in work function, surface termination, defect chemistry, oxidative stability, dispersibility and interfacial adhesion . In one study described, 23.6% efficiency was obtained on perovskite cells with carbon electrodes, by doping a hole-injection layer with graphene oxide [21]. This result validates a particular design of the interface, but does not prove that carbon-based nanomaterials are a generally cost-effective substitute for metallic contacts. Especially, MXene-containing device evaluations should provide surface chemistry, environmental stability and fabrication repeatability before asserting a general device-level advantage.

4.6 Quantum dots and other absorber systems

Colloidal semiconductor quantum dots offer size-dependent tunability of optical and electrical characteristics and can be deposited from solution. However, its technical translation is subject to surface imperfections, nanocrystal coupling, ink stability and broad area film homogeneity. Shi et al. [22] reported a PbS quantum-dot ink-engineering technique aiming to improve colloidal stability, printability and film formation. Related work in organic photovoltaics further demonstrates the broader applicability of nanoscale morphology management: a 2025 study showed 20.82% efficiency and tolerance to fluctuations in active-layer thickness by control of the crystallization sequence [23]. The latter result should be understood as evidence for nanoscale phase and shape engineering and not as an improvement due to a single nanoparticle additive.

Cross-technology comparisons will have to disentangle the contributions of device architecture, interfacial design and nanoparticle chemistry. Tandem efficiencies of 33-35% are determined by the linked optical, electrical and manufacturing features of whole devices rather than the effect of a single additive [1,11,12,13]. Similarly, independent certification of efficiency, champion-cell findings and area-normalized module performance are alternative populations of measurement. Therefore, there is a strong case for transparent area definitions, stabilizing methods, replicating statistics and assessment of system-level bottlenecks. For example, an effective passivation nanolayer may only enhance moderately at module scale if interconnection or contact patterning or encapsulation losses prevail. Table 1 presents a summary of representative PV-device and nanocoating experiments including their measured outcomes and comparison bounds.

Table 1. Selected primary PV and coating evidence, preserving original measurement boundaries.

PV function	Material / architecture	Reported study outcome	Evidence interpretation	Ref.
Silicon black texture	Black-silicon, passivated IBC	22.1% cell PCE (2015)	Highlights the importance of surface recombination control; not a current record	[2]
Si contact selectivity	Hybrid passivating back contacts	27.81% cell PCE; FF 87.55%	Certification status is not inferred from the reported cell result	[16]

PV function	Material / architecture	Reported study outcome	Evidence interpretation	Ref.
Tandem interface	Ultrathin LiF + molecular passivation	33.89% certified stabilized tandem PCE	Small-area cell; outcome reflects the complete tandem architecture and processing	[11]
Flexible tandem	ICO:H recombination + IZO transparent contacts	33.6% certified PCE; 91% after 5,000 bends	Mechanical and stability findings are specific to the reported protocols	[12]
Ambient coating	PNCC polymeric interface; blade coating	26.5% certified single junction; 33.0% tandem	Results concern distinct device formats; manufacturing yield is not evaluated	[13]
Quantum dots	Stabilized PbS quantum-dot ink	More uniform, printable CQD films	No efficiency comparison is presented without a matched area and reference	[22]
Carbon electrodes	Graphene-oxide-modified injection layer	23.6% reported cell efficiency	Specific carbon-electrode perovskite architecture	[21]
Module anti-soiling	Hydrophobic oxide/PDMS nanocomposite	~0.4% vs ~3.1% field efficiency loss	Seven-week outdoor exposure does not establish service lifetime	[24]

5. Nanostructured optical and anti-soiling coatings

Nanostructured front-surface coatings constitute a distinct intervention from modifications of the photovoltaic absorber or charge-transport layers. Silica-, titania-, and alumina-based formulations can alter surface wettability, particle adhesion, spectral transmission, and optical scattering. In dust-prone environments, their principal practical benefit may be the preservation of incident optical flux over time rather than an increase in intrinsic cell PCE. Appropriate characterization includes wavelength-resolved transmission and haze, contact-angle retention, surface topography, deposited dust mass, abrasion resistance, and electrical output relative to both soiled and cleaned uncoated controls. Without a properly cleaned reference, improved soiling resistance can readily be misidentified as a fundamental enhancement of energy-conversion efficiency.

In a 7-week outdoor study of PDMS/zinc/oxide nanocomposite coatings in 2026, efficiency losses due to dust were indicated to be about 0.4% for coated panels and 3.1% for untreated controls [24]. These values are specific to the reported exposure time, definition of measurement and comparator . Another study was conducted in 2026 to investigate SiO2 and TiO2 nanocoatings in weather conditions in Baghdad, which showed the need of coating research in hot and dusty regions [25]. Related work has been done on Al2O3 surfaces treated with oleic acid [26]. Taken together, these investigations justify rigorous field evaluation, but do not prove that short-term coating performance predicts multi-year resistance to ultraviolet exposure, abrasive sand, or recurrent washing.

Long-term coating performance is a result of the interaction between dust composition, moisture induced adhesion, mechanical abrasion and cleaning methods. Thus, site-representative experiments with local dust morphology and realistic humidity histories may provide more transferable evidence than contact-angle measures alone [27]. Testing of coatings is also needed on full glass–encapsulant–cell assemblies, as optical transmission, adhesion, thermal expansion and cleaning durability depend on the multilayer module structure. Commercial feasibility also demands considering the cost of deposition, the maintenance needed and the potential compatibility with existing module warranties.

The efficiency of anti-soiling coatings should be evaluated against uncoated modules with the same exposure and cleaning regimen. Surface wettability is an insufficient proxy for annual energy output. Wavelength-resolved transmission, haze, abrasion resistance and post-cleaning optical retention are also needed. Note that hydrophobicity or surface roughness may be increased to the detriment of adhesion or spectrum transmission. These opposing effects emphasize the necessity of simultaneous optical, mechanical, and electrical evaluation under representative operating conditions [24,25,26,27].

A useful time-resolved test of the anti-soiling mechanism is provided by an independently reported outdoor experiment (Fig. 3). Tayel et al. [28] reported on dust collection and PV conversion efficiency of matched coated and untreated panels over 40 days. The comparison provides a measurable field response but extrapolation to other climates or coating formulas is not recommended.

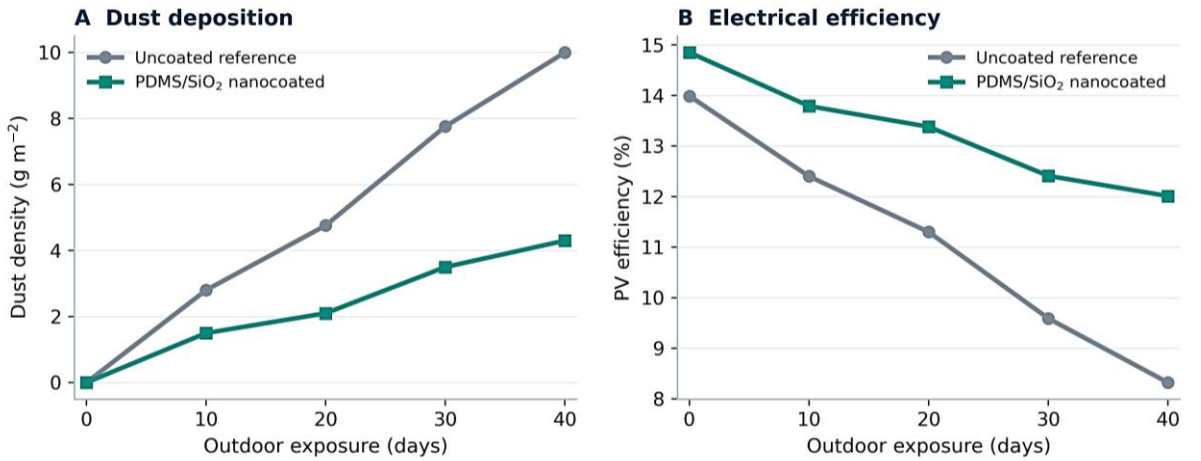


Fig. 3. Field evidence for PDMS/SiO_2 anti-soiling nanocoatings: (A) dust accumulation and (B) electrical conversion efficiency over 40 days. Source data for the two original reconstructed plots are explicitly reported by Tayel et al. [28].

6. Nano-enabled PVT heat transfer

6.1 PVT heat-removal pathways

Conventional PVT collectors employ water, water–glycol mixtures, or air in conjunction with bonded absorbers, serpentine flow passages, sheet-and-tube exchangers, or microchannels. To isolate the effect of a nanofluid, the primary comparator should be a water-cooled collector of identical design operated under matched flow and environmental conditions; an uncooled PV module provides a separate reference for the overall benefit of heat removal. Comparisons limited to nanofluid-cooled PVT and uncooled PV confound the addition of a cooling system with the particulate contribution. Where circulation is mechanically driven, the associated hydraulic electricity demand must be accounted for when reporting net electrical benefit.

6.2 Metal-oxide and hybrid coolants

Dispersions of CuO, Al_2O_3, TiO_2, ZnO, Fe_3O_4, and carbon-based materials have been investigated for improved PVT heat transfer. Compared to the stated uncooled and water/PCM references, an experimental system in 2024 that combined a CuO-water coolant with PCM storage achieved electrical-efficiency gains and a total energy efficiency of 82.1%. The greatest panel-temperature drop was 14.9 °C and the average efficiency gain was 16.8% under its defined comparison in a separate experimental research of MWCNT/ZnO-water cooling that took place in 2024 [30]. You can't generalize these findings to other materials because they are specific to certain experimental setups; factors like absorber design, operating temperatures, weather, and baseline selection all play a role.

6.3 Hybrid and ternary nanofluids

A controlled 2026 investigation compared single-component GO, TiO_2, and Fe_3O_4 dispersions with corresponding binary and ternary mixtures over mass flow rates of 20–80 kg h^{-1} and reported concentrations of 0–1%. For the tested collector, the GO/TiO_2/Fe_3O_4 ternary formulation achieved maximum energy and exergy efficiencies of 89.95% and 15.36%, respectively [31]. Because the formulations were assessed within a common apparatus, comparisons among those configurations are more defensible than rankings based on unrelated studies. In contrast, a 2024 numerical investigation predicted reductions of 11% and 13% in electrical exergy efficiency for Fe_2O_3 and TiO_2–Fe_2O_3 configurations, respectively, under its specified assumptions [4]. These findings need not be considered mutually inconsistent: they differ in formulation, collector design, comparator, modeling or experimental method, and

assessment boundary. Their combined significance is that first-law thermal or total energy efficiency cannot replace measurements of net electrical performance and exergy.

An additional experimental comparison enables stronger attribution of nano-coolant thermal gains (Fig. 4). Under the conditions evaluated by Sharaby et al. [32], water-cooled and MWCNT–ZnO-cooled PVT collectors achieved mean thermal efficiencies of 40.9% and 44.6%, respectively, while their reported peak efficiencies were 46.7% and 55.1%. The study used 0.2 mass% hybrid nanoparticles; the peak and daily-average metrics should be interpreted separately.

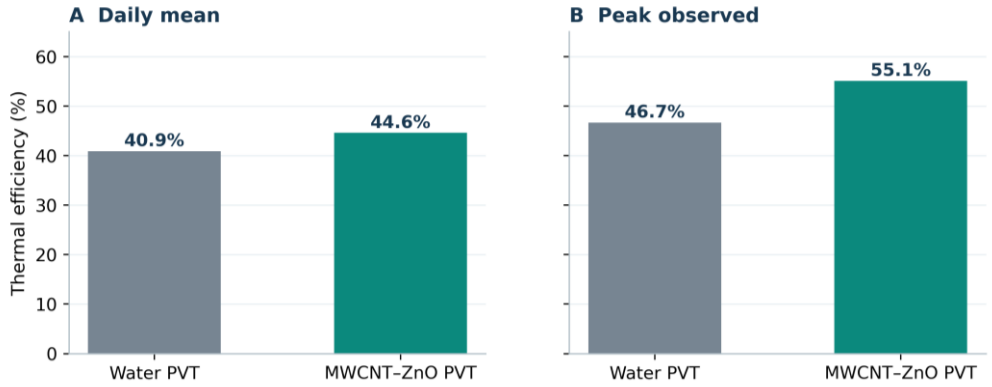


Fig. 4. Water-cooled versus 0.2 mass% MWCNT–ZnO hybrid-nanofluid PVT collector: reported daily mean and peak thermal efficiencies in the outdoor experimental study of Sharaby et al. [32].

6.4 The thermal-conductivity trap

Colloidal stability and rheological behavior are central determinants of nanofluid feasibility, not secondary formulation details. Although surfactants, pH adjustment, and surface functionalization may mitigate aggregation, they can also alter wettability, promote fouling, or increase pumping requirements. A 2025 investigation of PDMS/TiO_2 fluids documented changes in thermophysical characteristics following extended storage [5]. Although that work was not conducted in a PVT collector, it underscores the importance of time-dependent fluid characterization. Paliwal et al. examined concentration-dependent properties of Al_2O_3 dispersions for photovoltaic cooling [33], while additional work on multicomponent nanofluids addressed the simultaneous optimization of stability and thermophysical behavior [34]. Any claim of superior collector heat transfer should therefore be accompanied by appropriate measurements of viscosity, pressure drop, density, heat capacity, flow regime, and thermal boundary conditions.

The thermal–hydraulic trade-off is quantified by a published numerical PVT study (Fig. 5). Alktranee et al. [4] reported pressure-drop increases of 35.55% for 0.3 vol% Fe_2O_3 and 62.9–69.41% for 0.2–0.3 vol% TiO_2–Fe_2O_3 hybrids relative to water. These simulation-based penalties must not be interpreted as experimentally measured pumping energy or a universal fluid-property trend.

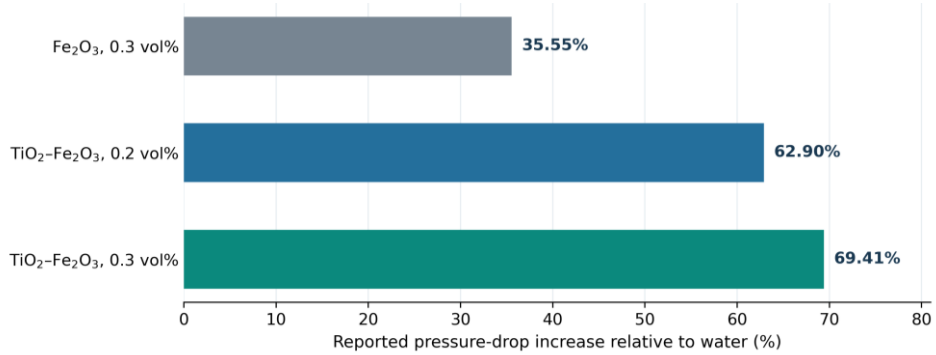


Fig. 5. Reported relative pressure-drop penalties in the Fe_2O_3 and TiO_2–Fe_2O_3 PVT numerical model. This comparison isolates within-study simulated formulations; it does not represent experimentally measured hydraulic losses [4].

6.5 Newer combined systems

In October 2026, an outside experiment on PVT systems combining MgO and ZnO-based nanofluids with phase-change storage was released. Under the tested conditions, the maximum overall energy efficiency was 50.17% for MgO–water–PCM configuration, while it was 43.74% for water-based PVT reference [35]. These efficiencies should not be compared with figures from unrelated studies without reconciling their energy-accounting standards, collector geometries and environmental circumstances. A relevant study to the Iraqi environment, the electrical efficiencies ranged between 12.8% and 13.5% over the experimental range for the MWCNT-assisted cooling paired with a spiral-flow absorber [36]. Taken together, our results support configuration- and climate-specific optimization, rather than a universal hierarchy of nanoparticle formulations.

Nanofluid concentration should be clearly expressed in unambiguous units and composition definitions. Mass fraction (wt%) and volume fraction (vol%) are not interchangeable without considering the densities of the constituents. Document viscosity and conductivity, density and specific heat, pressure loss and particle-size distribution, sedimentation after storage, and particle behavior after circulation, for reproducible assessment. Hydraulic-power is not accounted for in the optimization of concentration to provide a better net system advantage of higher apparent thermal efficiency. In the controlled mono-/binary-/ternary research [31] and the numerical exergy counterexample [4] the requirement for performance assessment within matched collectors rather than building rankings from disparate reported maxima is demonstrated.

7. Nano-enhanced PCM and spectral splitting

7.1 PCM as a thermal buffer

Latent-heat storage can smooth transient heating of the module by absorbing energy during the PCM melting time and releasing the stored heat as external conditions change. Importantly, traditional PCMs can provide benefits in the absence of nanofillers. An experiment conducted in 2025 for 47 days shown that the optimized PCM arrangement increased the generation of electrical energy by up to 6.84% and reduced the highest temperature at the back surface by 26 °C [37]. This conclusion serves as a required non-nano standard for later claims on particle additives. The combined effect of PCM thickness and coolant-flow conditions was investigated in a subsequent dual-channel PCM/PVT investigation [38].

7.2 What nanoparticle fillers actually change

The heat conductivity and crystallization behavior of the composite can be affected by graphite, graphene and chosen metal-oxide fillers. Their amount and direction rely on the particle morphology, the quality of the dispersion, the percolation behavior and the chemical compatibility with the storage medium. In 2025, an experimental investigation on boron-nitride/PCM composites investigated the influence of filler loading, phase-change composition, and geometrical arrangement; the optimal configuration had a reported electrical efficiency of 13.25% at a panel temperature of 37.58 °C [7]. These numbers are for that particular test arrangement and not some transferable performance ceiling. Therefore, the conductivity improvement should be considered together with the enthalpy of fusion, leakage, phase segregation, supercooling, cycling stability and the mass of the whole storage assembly.

7.3 Nanofluid–PCM combinations

The combination of PCM storage and coolant circulation could havebeneficial interactions, but also significant attribution problems. Regardless of the nanoparticle additive, improvements can be achieved by modifying exchanger shape, thermal mass, circulation energy or module installation. Studies on CuO nanofluids and PCM [29], nanofluid/NPCM with semicircular absorber tubes [39] or MgO dispersions with PCM [35] should thus be interpreted through factorial controls whenever possible, i.e. uncooled PV, water-cooled PVT, nanofluid-cooled PVT, water-cooled PVT with PCM and nanofluid-cooled PVT with PCM. For instance, a 2024 semicircular-tube research achieved electrical and thermal efficiencies of 12.70% and 78.99%, respectively, for its best-performing combination design at 5 L min^{-1} under increased ambient temperatures [39]. The finding is exclusive to the studied architecture and should not be compared directly with experiments performed at various irradiance or exchanger geometries.

7.4 Spectral splitting

spectrum-splitting PVT systems utilize wavelength-selective fluids or optical devices to steer appropriate photons toward the PV absorber, while other spectrum components are recovered as thermal energy. Their performance is highly dependent upon direct and diffuse irradiance, fluid absorptance, optical path length, concentration and long term filter stability. In 2025, a full scale outdoor investigation was conducted on a nanofluid based spectral-splitting system combined with PCM, reporting overall efficiency up to 28.4% for the configuration studied [14]. The numerical disparity between this figure and efficiencies reported for ordinary water-cooled collectors highlights why the definition of the efficiency numerator, energy border and useable thermal output must be set before comparisons of the results of other studies are undertaken.

The latent-heat capacity of nano-enhanced PCMs must be stated based on the mass of the complete composite, not on the mass of the unmodified PCM alone. Conductive additives may increase thermal charging and discharging, and reduce available latent storage per kg . More insulation may improve daylight retention, but inhibit subsequent release of heat . Controls containing only PCM, only nanoparticles (if applicable), and the combination nano-PCM formulation separate the individual contributions [7,37,38]. Spectral-splitting fluids need to be characterized optically on their own merit, as diverting absorbed radiation into useable thermal energy is not the same as boosting photovoltaic power generation [14]. Table 2 compares the relevant PVT, spectral-management and thermal-storage investigations, separating experimental data and numerical predictions .

Table 2. Experimental and numerical evidence for PVT, spectral-splitting and thermal-storage strategies.

Intervention	Evidence class	Reported outcome	Major comparability caveat	Ref.
CuO-water + PCM	Outdoor experiment	82.1% best reported total energy efficiency	Water/PCM and uncooled PV baselines; boundary dependent	[29]
MWCNT/ZnO-water	PVT experiment	Maximum ΔT 14.9 °C; average efficiency +16.8%	Improvement applies to the comparator and conditions of the original study	[30]
Nanofluid + NPCM	Semicircle absorber; experiment	ηe 12.70%, ηth 78.99% at 5 L/min	Collector geometry and ambient conditions limit cross-study comparability	[39]
GO/TiO_2/Fe_3O_4 ternary	Controlled experimental PVT	ηenergy 89.95%; ηexergy 15.36%	Within-study contrasts are more defensible than cross-study rankings	[31]
Fe_2O_3; TiO_2/Fe_2O_3	Numerical PVT model	Electrical exergy −11%; −13% in model	Numerical prediction; illustrates potentially adverse trade-offs	[4]
MgO-water + PCM	Outdoor experiment, 2026	Total efficiency 50.17% vs 43.74% water PVT	Efficiency boundaries differ from those adopted in other studies	[35]
BN-filled PCM	Composite optimization experiment	13.25% PV efficiency at 37.58 °C	Composite-specific configuration, not a universal optimum for PVT	[7]
Conventional PCM	47-day experiment; non-nano	Up to +6.84% electrical output; ΔT up to 26 °C	Essential non-nano comparator for isolating the added value of nanoparticles	[37]
Nanofluid spectral split + PCM	Full-scale outdoor experiment	Maximum total efficiency 28.4%	Optical and system boundaries differ from those of other studies	[14]

8. Material characterization and experimental quality assurance

A rigorous assessment of nano-enabled solar technologies requires explicit links between performance claims and experimentally measurable material properties. Particle size and morphology should be established using electron microscopy or suitable scattering techniques, accompanied by representative size distributions rather than nominal supplier specifications alone. Dispersion stability should be evaluated over relevant storage and circulation durations

through repeated property measurements, sedimentation analysis, zeta potential where appropriate, and examination of fouled components after testing. Coating studies should quantify wavelength-dependent transmittance, reflectance, absorptance, and haze before and after accelerated or natural exposure. For photovoltaic interfaces, chemical and electronic probes, including XPS/UPS, photoluminescence, impedance spectroscopy, and light-intensity-dependent open-circuit voltage, should complement calibrated current–voltage and external-quantum-efficiency measurements. PCM characterization should include differential scanning calorimetry, melting/freezing behavior, thermal conductivity, repeated cycling, and dimensional or shape stability [5,7,10,40].

Photovoltaic measurements should state the illuminated or aperture area, use of masks, voltage-scan direction and rate, stabilization procedure, and maximum-power-point tracking protocol. The ISOS consensus guidance for perovskite photovoltaics particularly emphasizes transparent reporting of exposure conditions, electrical loading, degradation metrics, and testing procedures [40]. PVT experiments require simultaneous monitoring of plane-of-array irradiance, inlet and outlet coolant temperatures, ambient temperature, module temperature, flow rate, pressure difference, and pumping electricity. Measurement uncertainty should be propagated through calculations of electrical efficiency, thermal efficiency, heat gain, and exergy. In dusty environments, coating assessments should additionally include repeated soiling and cleaning as well as moisture-dependent adhesion behavior [25,27].

Claims regarding combined nanofluid–PCM systems should be evaluated through factorial experimental designs rather than selected, unmatched reference cases. A minimum comparative matrix comprises an uncooled PV reference, a geometrically identical water-cooled PVT collector, a nanofluid-cooled collector, a water-cooled PVT/PCM arrangement, and a combined nanofluid–PCM arrangement. Where thermal storage operates without circulation, an additional PCM-only PV control may be necessary. All configurations must employ consistent definitions of illuminated area, irradiance, and operating conditions. Studies lacking uncertainty estimates, independent repeat measurements, or well-matched controls should be described as preliminary evidence rather than as conclusive demonstrations of system superiority.

Separation of physically separate interventions should also be a goal of the experimental matrix's design. When doing PV research, it is helpful to have untreated references and, if applicable, independent controls for the optical and chemical interfaces, with devices that can be replicated statistically. The impacts of particle addition, heat exchanger design, fluid flow parameters, and storage layout should be distinguished in PVT experiments. To ensure accurate comparisons and logically attributable performance gains, it is crucial to have independent replication, calibrate instruments, propagate uncertainty, and make raw time-series measurements publicly available.

9. Performance metrics, normalization and exergy

Where Pmax is the maximum electrical power, G is the incoming irradiance, and A is the clearly stated lighted or collector area, the basic electrical performance parameter is η_e=P_max/(G A). A consistent module-area definition and the actual operating temperature should be reflected in the electrical performance of PVT collectors, whereas cell-level measurements need the specification of the irradiation spectrum and cell temperature. The practical thermal output of a circulating PVT collector, under steady-state conditions, is Q̇u=ṁcp(Tout - Tin), which gives η_th=Q̇_u/(G A). When adding nanoparticles changes the specific heat capacity or other important parameters, it is important to test the fluid's correct qualities under typical operating conditions.

$$\eta_{\mathrm{e}} = \frac{P_{\max}}{G\,A} \tag{1}$$

$$\dot{Q}_{\mathrm{u}} = \dot{m}\, c_{\mathrm{p}}\, (T_{\mathrm{out}} - T_{\mathrm{in}}) \tag{2}$$

$$\eta_{\mathrm{th}} = \frac{\dot{Q}_{\mathrm{u}}}{G\,A} \tag{3}$$

$$P_{\mathrm{net}} = P_{\mathrm{PV}} - \frac{\Delta p\, \dot{V}}{\eta_{\mathrm{pump}}} - P_{\mathrm{aux}} \tag{4}$$

Net electrical performance must be defined at a transparent system boundary. The practical output can be expressed as $P_{net} = P_{PV} - P_{pump} - P_{aux}$, where the hydraulic contribution is $P_{pump} = \Delta p\ \dot{V}/\eta_{pump}$ when the relevant pump efficiency is known. A coolant-induced decrease in module temperature at a specified flow rate cannot establish a net benefit unless the associated pressure drop and electricity demand are also characterized. Performance changes should be reported both as an absolute efficiency difference, $\Delta\eta_e = \eta_e, new - \eta_e, reference$, in percentage points, and as a relative improvement, $[(\eta_e, new/\eta_e, reference) - 1] \times 100\%$. Thus, increasing electrical efficiency from 12% to 13% represents an absolute gain of 1 percentage point and a relative increase of approximately 8.33%, rather than a 1% relative increase.

The commonly reported first-law total PVT efficiency, $\eta_{total} = \eta_e + \eta_{th}$, is meaningful as a combined energy-accounting indicator only when both terms use compatible irradiance and area definitions. It does not imply that electrical work and recovered heat possess equivalent thermodynamic value. For a flowing coolant, useful thermal exergy can be evaluated through $\dot{m}[(h_{out} - h_{in}) - T_0\ (s_{out} - s_{in})]$, where T_0 is the ambient reference temperature and h and s denote specific enthalpy and entropy. For an idealized incompressible fluid with constant c_p, the thermal contribution is $\dot{m}c_p[(Tout - Tin) - T_0 ln(Tout/Tin)]$, with temperatures expressed in kelvin and pressure-related contributions neglected. Exergy-efficiency calculations should explicitly state whether electrical exergy, thermal exergy, and pumping demand are incorporated. This distinction helps explain why apparently favorable overall energy efficiencies may coexist with comparatively limited useful-energy quality [4,31].

This review does not combine the effect sizes of any studies. Convergent result definitions, uncertainty intervals, multiple measurements, and adequately comparable experimental circumstances are necessary for a statistically acceptable synthesis. The precise reference configuration, material composition, particle loading, PV/PVT architecture, flow conditions, environmental exposure, and matched within-study contrasts should be the near-term goals instead. Future quantitative synthesis would benefit from such uniformity since it would eliminate the possibility of deceptive rankings derived from maximum values isolated from studies that are not comparable. Because the exergy value of recovered heat varies with temperature, device PCE and first-law PVT collector efficiency are not equivalent metrics. The thermal exergy can be roughly expressed as Q̇u(1 - T_0/T_lm), where T_lm is a justified thermodynamic mean temperature of heat supply, under properly specified simplifying assumptions. Applying the inlet-to-outlet flow-exergy balance with particular enthalpy and entropy allows for a more thorough study. It is essential to use an absolute scale when expressing any thermodynamic temperature. To avoid double-counting of stored and discharged heat, performance should be integrated throughout the relevant time frame for transitory or seasonal operation. Tabulated in Table 3 are the bare minimums of reporting information and matched-control criteria needed to assess these metrics.

The distinction between electrical and useful thermal exergy is illustrated by the same experimentally tested systems (Fig. 6). Sharaby et al. [32] reported average electrical exergy efficiencies of 16.12% for the water-cooled and 16.8% for the hybrid-nanofluid collector, compared with thermal exergy efficiencies of 0.25% and 0.56%, respectively. The axes must remain separate because the two quantities differ markedly in magnitude; hydraulic auxiliaries and full-life costs require additional system-level analysis.

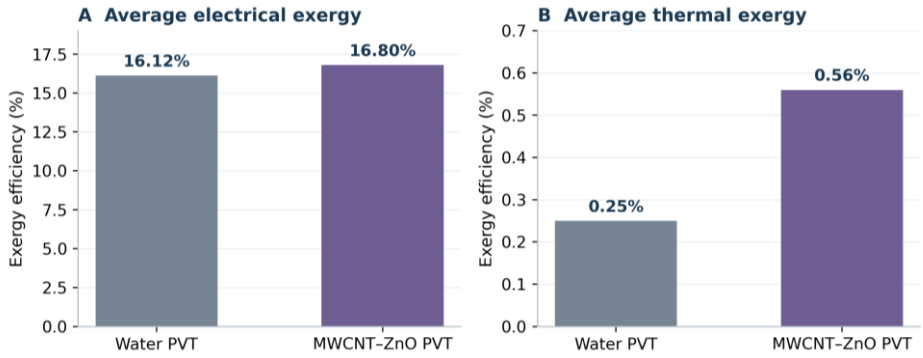


Fig. 6. Experimentally reported average electrical and thermal exergy efficiencies for water-cooled and MWCNT–ZnO-cooled PVT systems, displayed on distinct scales [32].

Table 3. Minimum reporting and matched-control requirements.

Test level	Required inputs and comparators	Preferred output indicators
PV cell or module	Aperture and illuminated area; G and spectrum; cell temperature; calibrated J–V/MPPT; Voc, Jsc, FF and EQE	Absolute PCE, stabilized PCE, daily or annual kWh, uncertainty
Nanostructured surface coating	Glass-control transmittance/haze; soiling chemistry; abrasive cleaning; UV/humidity cycling	Paired clean/soiled yield and optical retention
Nanofluid cooling	Particle loading basis; size; k, μ, cp, ρ; Tin/Tout; m_dot; Δp; pump electricity; aggregation	Net electrical gain, Quseful, exergy, drift over time
Nano-PCM system	Filler fraction; DSC enthalpy; melting/freezing curves; thickness; cycling; leakage	Charge/discharge energy, shifted PV temperature, total storage mass
Life-cycle and economic assessment	BOM, manufacturing energy, water use, nanoparticle recovery and end-of-life	LCOE or delivered energy cost and material burden

The collector-level balance between improved thermophysical properties and possible hydraulic or operational penalties is summarized schematically in Fig. 7.

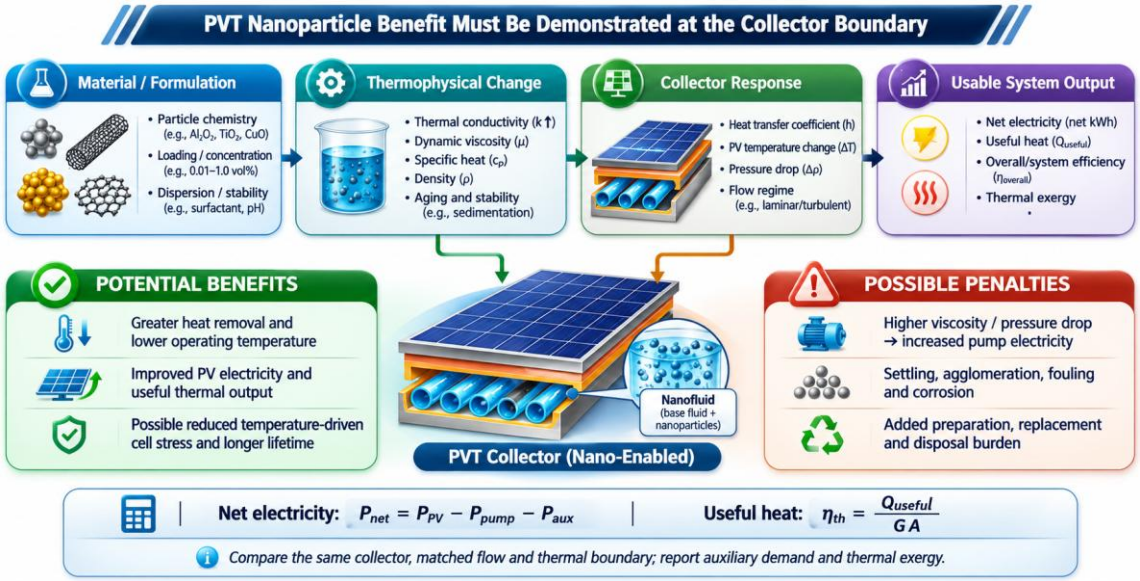


Fig. 7. Conceptual pathways linking nanofluid thermophysical properties to the benefits and penalties of PVT collector operation. No fitted trends or numerical experimental data are implied. Net electrical output accounts for pumping and auxiliary consumption, while recovered heat and exergy are assessed at explicitly defined delivery temperatures.

Fig. 7 highlights the necessity of evaluaing nanofluid performance at the collector boundary. Changes in viscosity and pressure drop may offset improvements in heat extraction, even when the convective heat-transfer coefficient increases. Joint reporting of pump-adjusted electrical output and useful heat supplied at a specified temperature provides a more defensible basis for evaluation than either instantaneous heat-transfer enhancement or nominal total energy efficiency alone [4,30,31]. The complementary assessment boundaries at the PV-device, PVT-collector, and whole-life levels are presented in Fig. 8.

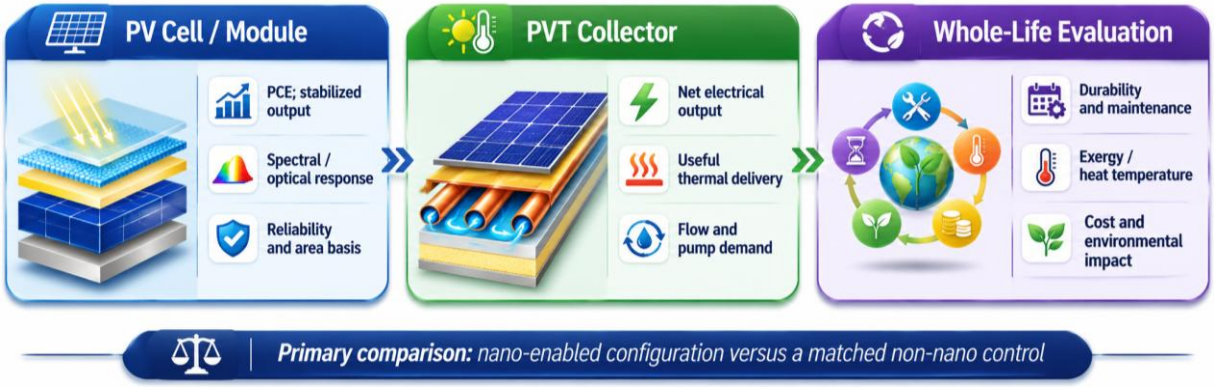


Fig. 8. Proposed cross-scale assessment boundaries and associated performance indicators for PV devices, PVT collectors, and whole-life system evaluation. Original conceptual schematic without numerical data.

10. Critical comparison and research implications

The studies summarized in Table 1 address fundamentally different performance constraints. At the device level, interfacial defect passivation and carrier-selective contact engineering have produced major gains in independently verified PV efficiency [10,11,12,13,16]. In PVT collectors, the principal near-term objectives are reduced module temperature and increased useful thermal recovery without disproportionate pumping demand; however, the supporting studies frequently involve relatively short laboratory or outdoor campaigns [4,29,30,31,35,39]. For module-front coatings, the relevant benefit is often preservation of optical access during soiling exposure, which may be especially important in arid environments [24,25,27]. These endpoints represent distinct physical and system functions and cannot be substituted for one another.

Evidence from nanofluids is most useful when compared across different formulations evaluated using the same collector and measurement technique; this is demonstrated in the 2026 mono-/binary-/ternary study [31]. On the flip side, generalized enhancement claims should be qualified by the numerically projected exergy drop related with nanoparticle addition [4]. However, it is vital to note that these findings should be identified as modeled, not empirically seen. While conventional-PCM results [37] show that significant gains may already be achieved without additives, the nano-enhanced optimization study [7] provide proof regarding modified storage qualities in PCM research. Therefore, the important thing to consider is whether a nanomaterial offers a consistent improvement over the most viable alternative that does not include nanotechnology.

Maximum efficiency or highest instantaneous temperature reduction under ideal test conditions is often highlighted in publications. Annual net electrical production, useful thermal delivery at a defined temperature, fraction of recovered heat that is actually utilized, storage discharge effectiveness, long-term component reliability, manufacturing burdens, and economic performance are better indicators for engineering decisions. Even when a system has a high first-law total efficiency, it doesn't mean it's practical. For example, if there's no need for low-temperature heat, it could be less helpful than a system that delivers less heat at a useful temperature with lower auxiliary consumption. Conclusions drawn from comparisons within studies are the strongest in the current body of evidence. While research on tandem cells [11,12,13] shows that optimized interfaces have an impact on high-efficiency device designs, Savin et al. [2] proved that contemporaneous surface passivation is important in optically textured silicon. Sharaby et al. [30] found that the tested configurations for PVT applications reduced panel temperature by a high of 14.9 °C and improved efficiency by an average of 16.8%. For their preferred ternary dispersion, Shahsavar and Toghraie [31] found an exergy efficiency of 15.36% and a peak energy efficiency of 89.95%. A universal material ranking cannot be established by these results due to the fact that the underlying collector geometries, hydrodynamic circumstances, comparators, and efficiency standards vary. Incorporating negative outcomes into a balanced critical synthesis is further supported by the contradictory numerical exergy results published by Alktranee et al. [4]. Based on this knowledge, Table 4 creates an engineering choice matrix that connects the main technological paths to their respective limits and validation needs.

Table 4. Critical engineering decision matrix: evidence strength, trade-offs and translation requirements.

Route	Evidence status	Dominant limitation	Required validation
Passivating nanolayers	Relatively strong: controlled device-level evidence	Stability, area scaling, manufacturing compatibility	Replicate devices; certified PCE; aging and yield distributions
Anti-soiling nanocoatings	Moderate: predominantly short-term field evidence	Dust chemistry, transparency and abrasion	Paired exposure, clean-state optics and cleaning-cycle durability
Single/hybrid nanofluids	Moderate: controlled collector-level evidence	Viscosity, pumping, dispersion, corrosion	Matched water baseline; hydraulic power; extended circulation
Nano-enhanced PCM	Emerging: composite and system-level comparisons	Latent-heat dilution, cycling and incomplete regeneration	PCM-only baseline; cycling; full-mass thermal storage
Spectral nanofluids	Emerging: outdoor prototype demonstrations	Electrical–thermal spectral trade-off	Spectra; separate electrical/thermal exergy; full annual yield

11. Reliability, manufacturing, cost and environmental considerations

A performance improvement that cannot be sustained under relevant operating conditions has limited engineering significance. Exposed nanostructured surfaces may undergo ultraviolet degradation, dust abrasion, and moisture-assisted damage. Perovskite interfaces can experience chemical reactions, ion migration, and thermally or photoinduced degradation. Circulating nanofluids may exhibit aggregation, channel fouling, corrosion, or pump deterioration, while nano-enhanced PCMs can suffer leakage, segregation, incomplete phase transitions, or capacity loss. Validation should therefore address relevant combinations of thermal cycling, damp heat, mechanical loading, UV exposure, stagnation, freeze protection where applicable, circulation endurance, and material recovery. IEC 61215 provides a relevant module-qualification framework but should not be treated as a direct predictor of the field lifetime of every novel nano-enabled configuration [40,41].

Having open and visible material and process inventories is crucial for manufacturing scalability. The following criteria should be used to assess nanocoatings: optical retention, cleaning or replacement costs, throughput, precursor or solvent consumption per square meter, and method of deposition. Analysis of nanofluids should detail the following: particle mass per collector, energy required for preparation, stability of circulation, replenishment intervals, filtering needs, corrosion, and disposal protocols. Useful latent heat per kilogram of the total assembly, containment mass, and retention after repeated cycles are the pertinent quantities for nano-enhanced storage. Research on PbS quantum-dot inks and ambient-fabricated perovskite devices [13,22] has highlighted the need for solution-deposited nanocrystal absorbers to meet certain criteria, such as ink shelf life, batch repeatability, compatibility with drying and annealing, and large-area homogeneity.

An open life-cycle inventory, not just the renewable energy application, is needed to back up claims of environmental benefit. Nanoparticle manufacturing, metal-oxide processing, surfactant chemistry, potential particle release, lead management in relevant absorber technologies, pump replacement, and end-of-life recovery are all important contributions. An example of integrated evaluation that did not require showing economic feasibility across different markets is one experimental inquiry from 2026 that evaluated improved PVT performance using techno-economic analysis [42]. Relying on yearly net electricity and useable thermal energy delivered at specified temperatures instead of nanoparticle purchase price or short-duration efficiency gains should be the standard for future comparative datasets regarding costs and environmental impacts.

The discrepancy between the theoretical potential and practical application becomes even more apparent when transient thermal advantages are considered long-term system benefits. There are a number of tests that need to be

performed on nanocoatings, circulatory fluids, and nano-enhanced PCMs. These tests are necessary following UV exposure, dust abrasion, and repetitive cleaning, as well as thermal aging, sustained pumping, sedimentation, and corrosion. The cost of nanoparticles should not be considered independently of the incremental levelized cost or payback for provided energy and temperature-qualified usable heat if economic comparisons are to be meaningful. Responsible deployment evaluations should also include material recovery, disposal, and release. The failure modes are connected to material-specific validation methodologies and evidence of performance retention, as shown in Fig. 9.

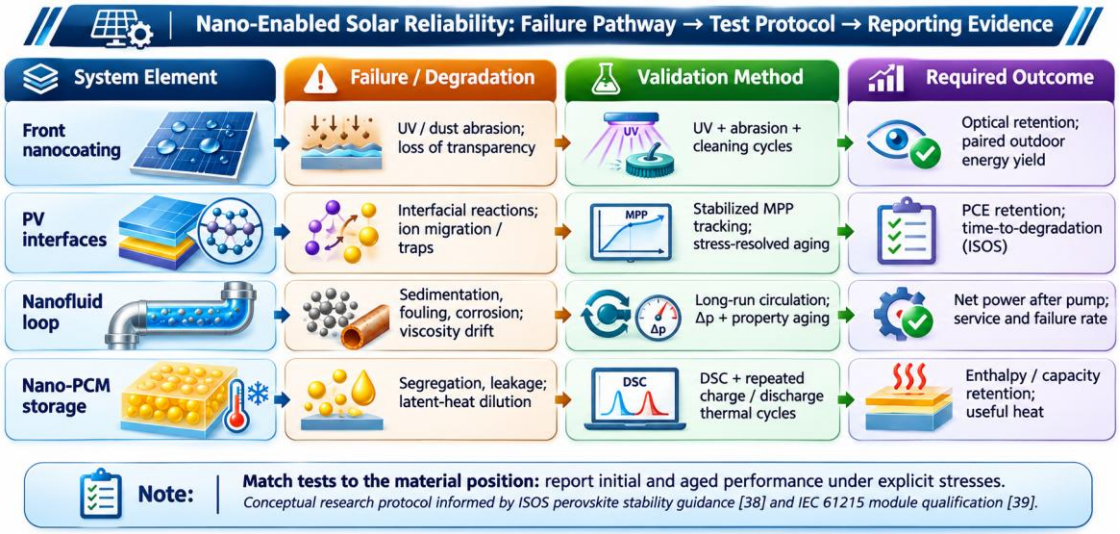


Fig. 9. Proposed reliability evidence map for nano-enabled PV/PVT systems, linking material-specific failure pathways to test protocols and performance-retention indicators. The framework is informed by perovskite stability reporting guidance [40] and crystalline-silicon module qualification guidance [41]; this is an original conceptual schematic.

As shown in Fig. 9, validation should be tailored to the functional location of each nano-enabled component. Anti-soiling coatings require assessment of optical retention and abrasion resistance; photovoltaic interfaces require stabilized power tracking and controlled aging studies; nanofluid loops require prolonged circulation, pressure-drop monitoring, and corrosion assessment; and nano-enhanced PCMs require repeated thermal cycling and measurement of latent-heat retention. Short accelerated tests can identify failure mechanisms but cannot, without additional evidence, establish long-term field service life [40,41].

12. Research roadmap and future perspectives

Step one: create reference configurations that are functionally identical. Instead of using a nominal baseline with varying passivation, processing, or optical geometry, every inquiry into PV nanomaterials should incorporate a nearly identical control that differs just in the intervention of interest. An identical water-cooled collector with the same absorber geometry and flow conditions should be reported in PVT nanofluid studies. To determine how much of an impact each component has in a combined nanofluid-PCM system, factorial controls are necessary. To increase causal attribution and prevent overstatement of nanoparticle-specific effects, one of the most immediate options is to systematically use matched baselines.

Objective No. 2: conduct field measurements with a focus on long-term uncertainty. Accurate and reliable outdoor methods should include measurements of hydraulic electricity, plane-of-array irradiance, usable heat supply, temperature distribution, documented cleaning procedures, and calibrated current-voltage or maximum-power-point readings. To capture all possible conditions, including start-up transients, low irradiance, dust occurrences, and stagnation, sampling should go beyond peak midday. Field investigations comparing self-cleaning coatings, traditional water-cooled PVT, and stable low-concentration nanofluids under matched daily or seasonal conditions would provide valuable information for hot and dry countries like Iraq [25,27,36].

Objective No. 3: seek out multiphysics optimization with physical constraints. Coupling optical approaches with

computational fluid dynamics, thermal network analysis, and finite difference time domain with transfer matrix modeling and ray tracing is recommended for certain architectures. To avoid exaggerating prediction generalizability, data-driven models necessitate quantified training datasets and validation procedures that disentangle formulations, devices, or environmental factors. Consequently, optimization should take into account a multi-objective trade-off involving operational stability, net electricity, installation cost, environmental risk, and useful thermal exergy. Possible design factors include particle morphology and concentration, exchanger geometry, and PCM thickness; explicit restrictions include pumping demand and suspension stability.

The fifth priority is to determine whether the technology is ready to grow and how to responsibly scale it up. There are well-established trends in high-efficiency PV production that are in line with the development of texturing that is compatible with industrial use, contacts that passivate, and interfaces that are nanoscale carrier-selective [3,10,11,12,13,16]. There is a need for compelling evidence regarding long-term fouling, particle release, hydraulic durability, sealing, and maintenance for the experimentally established prospects of nanofluid cooling and nano-enhanced PCM storage [5,7,31,42]. Laboratory formulations that rely on costly precursors, extremely tiny device areas, or unsubstantiated lifetime predictions are less believable than scalable coating and encapsulation processes when it comes to implementation.

There are five interconnected steps in the decision-making framework that emerges. One must first determine whether a combination supply, usable heat, or electricity is the necessary energy service. Secondly, the primary physical constraint is recognized, be it mechanical, electrical, optical, or storage-related. Third, we choose the right material composition and where to put the functions. Finally, a matched non-nano design is used to evaluate the suggested intervention. At last, within consistent system boundaries, the effects on exergy, dependability, cost, and the environment are considered alongside the benefits that have been documented. This structure is put into action in Fig. 10 and the tables that go along with it. Due to the intrinsic dependence of additive efficacy on mechanism, architecture, and application, no universal superiority ranking is suggested for TiO_2, ZnO, graphene, MWCNTs, or any other additive.

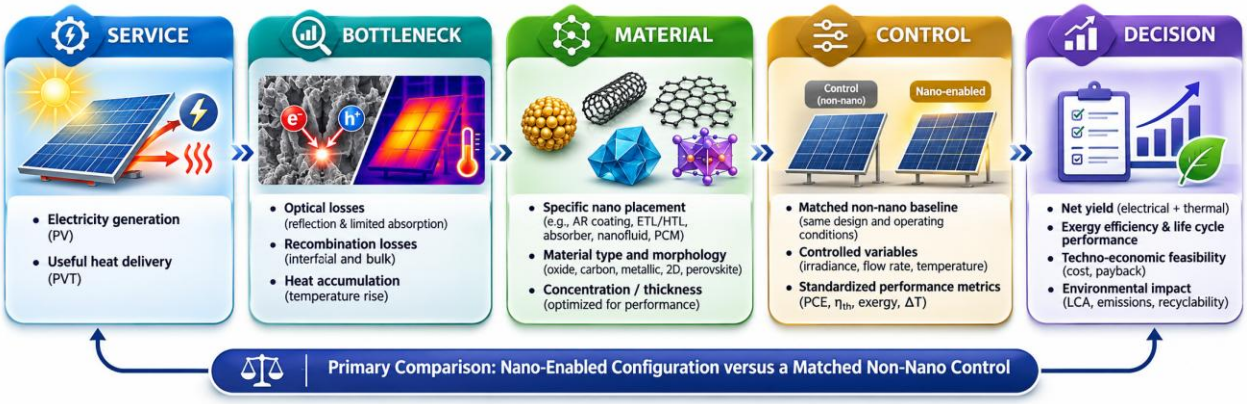


Fig. 10. Proposed evidence-to-deployment decision hierarchy for nano-enabled solar technologies, linking functional requirements, material selection, matched controls, and whole-life performance evaluation. Original conceptual framework.

13. Conclusions

Based on what we have seen so far, nanomaterials are more of a design enabler than a performance booster in and of itself. Improved device engineering and high conversion efficiencies have been greatly enhanced by controlling surface roughness, carrier-selective contacts, absorber morphology, and interfacial passivation on a nanoscale in photovoltaic devices. Under certain operating conditions, PVT systems can achieve measurable thermal or electrical gains with the help of nanofluids, conductive fillers, functional coatings, and integrated storage. Nevertheless, it is not enough to deduce their incremental contribution from material attributes or compare them with uncooled PV; they must be proven against suitable water-cooled and non-nano PCM controls. Instead of focusing solely on peak temperature reductions or aggregate first-law efficiency, scientifically valid performance evaluation should take into account stabilized electrical output, usable heat, exergy, uncertainty, operational durability, and auxiliary-energy-adjusted net output.

There has to be a focus on paired experimental designs, extended operational monitoring, clear uncertainty budgets, scalable manufacture, complete life-cycle evaluation, and independently validated device measurements in future research. Optimizing integrated solutions for sustained optical access, effective heat recovery, manageable hydraulic demand, and environmental exposure is more likely to yield promising results than randomly increasing nanoparticle concentration in hot and dust-prone environments. The groundwork for future quantitative synthesis might include a standardized, publicly available library of material compositions, matched controls, operating circumstances, and aged system performance. To ascertain whether particular PV and PVT configurations offered by nanotechnology offer long-term, economically plausible benefits over established non-nano alternatives, such proof is required.

References

[1] M.A. Green, E.D. Dunlop, M. Yoshita, N. Kopidakis, K. Bothe, G. Siefer, J.Y. Jiang, Solar cell efficiency tables: Version 68, Joule 10 (2026) 102494. https://doi.org/10.1016/j.joule.2026.102494

[2] H. Savin, P. Repo, G. von Gastrow, et al., Black silicon solar cells with interdigitated back-contacts achieve 22.1% efficiency, Nat. Nanotechnol. 10 (2015) 624–628. https://doi.org/10.1038/nnano.2015.89

[3] T.G. Allen, J. Bullock, X. Yang, et al., Passivating contacts for crystalline silicon solar cells, Nat. Energy 4 (2019) 914–928. https://doi.org/10.1038/s41560-019-0463-6

[4] M. Alktranee, Q. Al-Yasiri, K.S. Mohammed, H. Al-Lami, P. Bencs, Energy and exergy assessment of a photovoltaic-thermal (PVT) system cooled by single and hybrid nanofluids, Energy Convers. Manage. X 24 (2024) 100769. https://doi.org/10.1016/j.ecmx.2024.100769

[5] I. Carrillo-Berdugo, M. Gragera-García, S. Gragera-García, et al., Stability is the key for nanofluids to enter applications: Reflections from a case study on PDMS/TiO2 nanofluids, Therm. Sci. Eng. Prog. 59 (2025) 103288. https://doi.org/10.1016/j.tsep.2025.103288

[6] Madhi, H., Aljabair, S.; Imran, A. A. A review of photovoltaic/thermal system cooled using mono and hybrid nanofluids. International Journal of Thermofluids 22 (2024), 100679. https://doi.org/10.1016/j.ijft.2024.100679

[7] W. Zhou, Y. Wei, D. Wan, Experimental study and optimization the performance of photovoltaic panels using composite of phase change materials and boron nitride nanoparticles, J. Energy Storage 112 (2025) 115526. https://doi.org/10.1016/j.est.2025.115526

[8] A. Al Miaari, H.M. Ali, Recent advances on nano-enhanced phase change materials (NEPCMs) for photovoltaic thermal management and role of machine learning: A review of fundamentals, preparation, characterization, and thermo-physical properties, J. Energy Storage 124 (2025) 116544. https://doi.org/10.1016/j.est.2025.116544

[9] H.A. Atwater, A. Polman, Plasmonics for improved photovoltaic devices, Nat. Mater. 9 (2010) 205–213. https://doi.org/10.1038/nmat2629

[10] H. Min, D.Y. Lee, J. Kim, et al., Perovskite solar cells with atomically coherent interlayers on SnO2 electrodes, Nature 598 (2021) 444–450. https://doi.org/10.1038/s41586-021-03964-8

[11] J. Liu, Y. He, L. Ding, et al., Perovskite/silicon tandem solar cells with bilayer interface passivation, Nature 635 (2024) 596–603. https://doi.org/10.1038/s41586-024-07997-7

[12] S. Wang, W. Li, C. Yu, et al., Flexible perovskite/silicon tandem solar cells with 33.6% efficiency, Nature 649 (2026) 59–64. https://doi.org/10.1038/s41586-025-09849-4

[13] L. Wang, X. Hu, B. Niu, et al., Scalable ambient fabrication of single-junction and perovskite–silicon tandem solar cells, Nat. Sustain. (2026). https://doi.org/10.1038/s41893-026-01916-6

[14] M. Kumar, S. Kumar, S. Singh, N. Chander, A. Kumar, Outdoor thermal performance study of a full-scale nanofluid based spectral beam splitting photovoltaic/thermal system with phase change material, J. Energy Storage 140 (2025) 118909. https://doi.org/10.1016/j.est.2025.118909

[15] B. O'Regan, M. Grätzel, A low-cost, high-efficiency solar cell based on dye-sensitized colloidal TiO2 films, Nature 353 (1991) 737–740. https://doi.org/10.1038/353737a0

[16] G. Wang, M. Yu, H. Wu, et al., Silicon solar cells with hybrid back contacts, Nature 647 (2025) 369–374. https://doi.org/10.1038/s41586-025-09681-w

[17] C. Duan, K. Zhang, Z. Peng, et al., Durable all-inorganic perovskite tandem photovoltaics, Nature 637 (2025) 1111–1117. https://doi.org/10.1038/s41586-024-08432-7

[18] R. Lin, H. Gao, J. Lou, et al., All-perovskite tandem solar cells with dipolar passivation, Nature 648 (2025) 600–606. https://doi.org/10.1038/s41586-025-09773-7

[19] Li, R., Zhang, D., Wei, J., et al. n-type regulation of 2D perovskite interlayers for efficient perovskite-silicon tandem solar cells. Joule 9 (2025), 102141. https://doi.org/10.1016/j.joule.2025.102141

[20] Y. Song, X. Cai, S. Liu, et al., Air-processed perovskite/silicon tandem solar cells via iodide oxidation suppression, Adv. Mater. 38 (2026) e74786. https://doi.org/10.1002/adma.74786

[21] Y. Wang, W. Li, X. Wu, et al., Graphene oxide doping of the hole injection layer enables 23.6% efficiency in perovskite solar cells with carbon electrodes, Nat. Energy 11 (2026) 47–57. https://doi.org/10.1038/s41560-025-01893-8

[22] G. Shi, X. Ding, Z. Liu, et al., Overcoming efficiency and cost barriers for large-area quantum dot photovoltaics through stable ink engineering, Nat. Energy 10 (2025) 592–604. https://doi.org/10.1038/s41560-025-01746-4

[23] H. Chen, Y. Huang, R. Zhang, et al., Organic solar cells with 20.82% efficiency and high tolerance of active layer thickness through crystallization sequence manipulation, Nat. Mater. 24 (2025) 444–453. https://doi.org/10.1038/s41563-024-02062-0

[24] N. Sathiesh Kumar, D. Barik, Self-cleaning behaviour of hydrophobic nanocoating for solar PV panels: Enhancing efficiency and thermal management in dusty environments, Energy Reports 15 (2026) 109030. https://doi.org/10.1016/j.egyr.2025.109030

[25] A.A. Khudhur, H.K. Jobair, Investigation of the effects of SiO2 and TiO2 nanocoatings on photovoltaic module performance under Iraqi meteorological conditions, J. Eng. (Iraq) (2026). https://doi.org/10.31026/j.eng.2026.10.09

[26] M. Arslan, İ. Deveci, C. Arslan, et al., A new anti-soiling approach based on oleic acid-modified Al2O3 nanocoatings for photovoltaic panels, Sci. Rep. 16 (2026) 7615. https://doi.org/10.1038/s41598-026-38041-5

[27] J.A. Tsanakas, J.P. Rakotoniaina, J. Montoya, et al., Assessment of soiling dynamics and cleaning efficiency for photovoltaic modules under different dust environments, Solar RRL 10 (2026) e202500792. https://doi.org/10.1002/solr.202500792

[28] S.A. Tayel, A.E. Abu El-Maaty, E.M. Mostafa, Y.F. Elsaadawi, Enhance the performance of photovoltaic solar panels by a self-cleaning and hydrophobic nanocoating, Scientific Reports 12 (2022) 21236. https://doi.org/10.1038/s41598-022-25667-4

[29] M.A. Almeshaal, A.A. Altohamy, et al., Experimental analysis of a photovoltaic thermal collector using phase change materials and copper oxide nanofluid, J. Energy Storage 93 (2024) 112265. https://doi.org/10.1016/j.est.2024.112265

[30] M.R. Sharaby, M.M. Younes, F.S. Abou-Taleb, F.B. Baz, The influence of using MWCNT/ZnO-water hybrid nanofluid on the thermal and electrical performance of a photovoltaic/thermal system, Appl. Therm. Eng. 248 (2024) 123332. https://doi.org/10.1016/j.applthermaleng.2024.123332

[31] A. Shahsavar, D. Toghraie, Experimental comparison of energy and exergy performances of photovoltaic/thermal systems containing mono, hybrid, and ternary nanofluids, Sol. Energy Mater. Sol. Cells 296 (2026) 114065. https://doi.org/10.1016/j.solmat.2025.114065

[32] M.R. Sharaby, M.R. Sharaby, M.M. Younes, F.S. Abou Taleb, F.B. Baz, The impact of hybrid nanofluid cooling on photovoltaic/thermal system performance: a 3E analysis approach, Journal of Thermal Analysis and Calorimetry 150 (2025) 19575–19589. https://doi.org/10.1007/s10973-025-14889-z (see also correction: https://doi.org/10.1007/s10973-026-15280-2)

[33] Paliwal, M. K., Jakhar, S., Dhurandher, B. K.; Sharma, V. Experimental investigation on preparation, characterization and stability of Al_2O_3 nanofluid in application of PV thermal management. Environmental Progress & Sustainable Energy 44 (2025), e14648. https://doi.org/10.1002/ep.14648

[34] Babar, H., Wu, H., Zhang, W., Asim, M.; Koşar, A. Synergistic approach to colloidal stability and thermophysical optimisation of multi-walled carbon nanotubes, aluminium nitride, and silver-based hybrid nanofluids. Powder Technology 465 (2025), 121348. https://doi.org/10.1016/j.powtec.2025.121348

[35] M. Gamal, I. Mohamed, M. Abd El-Hamid, Experimental investigation of a photovoltaic/thermal system utilizing nanofluids incorporated with phase change materials, Sol. Energy 317 (2026) 114994. https://doi.org/10.1016/j.solener.2026.114994

[36] H.A. Kazem, M.T. Chaichan, Energy and exergy evaluation of photovoltaic thermal (PVT) system cooled by nanofluid and spiral flow absorber, Sohar Univ. J. Eng. Inf. Technol. Innov. 2 (2026) 20–32. https://doi.org/10.69983/sujeiti/2242

[37] D. Mazzeo, E. Ogliari, A. Lucchini, et al., Integration of photovoltaic modules with phase change materials: Experimental testing, model validation and optimization, Energy 319 (2025) 134959. https://doi.org/10.1016/j.energy.2025.134959

[38] F. Yuan, Z. Yin, N. Zhao, Y. Hu, J. Wang, Experimental and numerical analysis of phase change material-based photovoltaic/thermal system with dual-parallel cooling channels, Sol. Energy Mater. Sol. Cells 286 (2025) 113563. https://doi.org/10.1016/j.solmat.2025.113563

[39] M.M. Maseer, F.B. Ismail, H.A. Kazem, et al., Performance enhancement of photovoltaic/thermal collector semicircle absorber tubes using nanofluid and NPCM, Renew. Energy 233 (2024) 121152. https://doi.org/10.1016/j.renene.2024.121152

[40] M.V. Khenkin, E.A. Katz, A. Abate, et al., Consensus statement for stability assessment and reporting for perovskite photovoltaics based on ISOS procedures, Nat. Energy 5 (2020) 35–49. https://doi.org/10.1038/s41560-019-0529-5

[41] IEC, IEC 61215-1-1:2021, Terrestrial photovoltaic (PV) modules – Design qualification and type approval – Part 1-1: Special requirements for testing of crystalline silicon photovoltaic (PV) modules, International Electrotechnical Commission, Geneva, 2021. https://webstore.iec.ch/en/publication/61346

[42] M.M.A. Saeed, A. Ameen, Energy, exergy, and techno-economic performance of an enhanced photovoltaic/thermal collector, Solar 6 (2026) 62. https://doi.org/10.3390/solar6050062